Group versus phase velocity in laboratory measurements on orthorhombic samples

Robert W. Vestrum and R. James Brown

ABSTRACT

In laboratory measurements of traveltimes across anisotropic materials, there can be a significant difference between the group and phase velocities when the measurements are made in an off-symmetry direction. Ideally, to measure group velocity one should use waves generated by a point source and recorded with a point receiver; and one should use plane waves to measure phase velocity. In the actual laboratory condition we are dealing with an intermediate situation. There is some question, therefore, as to which of group or phase traveltimes across the medium in these directions is measured.

Forward models have been generated showing the wavefronts propagating through Phenolic CE, an orthorhombic-isotropic medium currently used in physical modelling experiments at The University of Calgary. These models have been interpreted and an assessment has been made to determine whether the traveltimes will invert to yield phase or group velocities or, in fact, something between the two. Further geometrical analysis has revealed an additional method of determining true group and phase velocities from the observed traveltimes.

From the modelling and geometrical analysis, it was determined that traveltimes due to phase velocity of the phenolic were measured in most of the off-symmetry-axis measurements reported by Cheadle et al. The group velocity appears difficult to determine given the finite size of the source and receiver transducers and the dimensions of the samples that were used.

INTRODUCTION

Physical modelling experiments have been performed by Cheadle et al. (1991) on the Phenolic CE which was found to have orthorhombic symmetry. In such experiments, transit times across a sample are measured with the goal of calculating velocities in the material which are then used to calculate the stiffnesses of the material. The question arises, however, as to whether the velocities determined in the normal way, i.e. by dividing distance between the transducer faces by traveltime, are group velocities, phase velocities, or some combination thereof.

Any dynamic effects investigated in this study of the source and receiver finiteness are only in the transit times. The only important observations that are made are the elapsed time between the excitation of the source and the first pulse arrival at the receiver and the distance between source and receiver.

THEORY

The question of group or phase velocities arises from the wave effects due to the source and receiver transducer sizes. In the case of a plane seismic wave propagating through a solid, the traveltime measured across the sample in the direction normal to the wavefront will be the phase velocity. With a wave propagating from a point source, the group or energy velocity will be measured in any direction away from that source. With the finite transducer source and receiver that is used in physical modelling work, there will be some portion of the wavefront that is flat like a plane wave and the rest of the wave surface will be in the shape of the group-velocity surface.

The orthorhombic medium has, by definition, three mutually perpendicular axes of symmetry. There is symmetry under any rotation of 180° about a symmetry axis, i.e. two-fold symmetry. In these symmetry directions, which were chosen for three of the six measurement directions, the group and phase velocities are equal.

Figure 1 shows an example of the difference between group and phase velocity in terms of the propagation of the wavefront in an anisotropic medium. The diagram shows two wavefronts in space that are separated by unit time. The distance that the wavefront has travelled along a particular ray emanating from the source in unit time is labelled ***g***, for group velocity. The normal distance between the two wavefronts is labelled ***v***, for phase velocity.

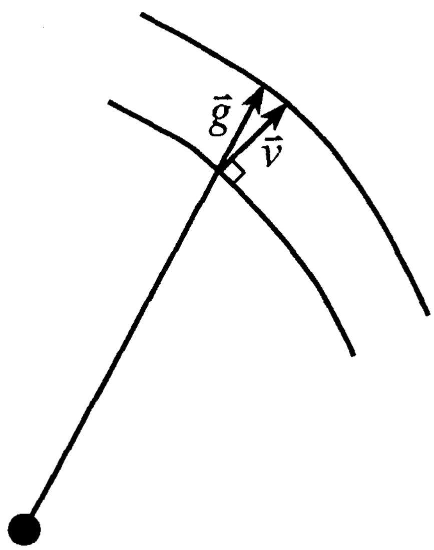

FIG. 1. Two wavefronts separated by unit time. The distances ***v*** and ***g*** travelled during that unit time represent the phase and group velocities respectively.

Figure 2 shows a plot of the wave propagating away from a relatively large source transducer. The group-velocity vector, labelled here as ***g***, represents the velocity of energy transport outward from the source. The vector ***v*** in white is the phase or normal velocity vector and shows the velocity of the plane wave across the sample in the direction normal to the wavefront. In this example the source and receiver diameters are 4 cm and the distance between the centres of their faces is 14 cm.

It can be seen for this sample (figure 2) that the transit time recorded and normal separation measured will yield phase velocity across the sample. That is, the first pulse arriving at the receiver will be from the plane-wave portion of the wavefront. If the receiver transducer had been located a bit to the left in the figure so that the displacement between its centre and the source were in the direction of ***g***, the transit time would represent the group-velocity. For receiver locations at some distance to the right of that shown (figure 2), the group-velocity will be in the direction from the right edge of the lower transducer to the left edge the receiver transducer and its magnitude is calculated by dividing the distance between these points by the traveltime.

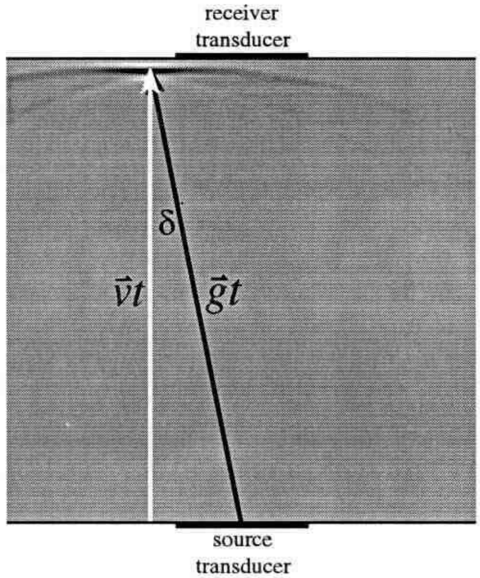

FIG. 2. Group and phase velocities of a wave propagating through the orthorhombic Phenolic CE. The white vector, labelled ***vt***, represents normal distance travelled by the wave moving at the phase or normal velocity in time *t* whereas ***g*** is the corresponding group or energy velocity and ***gt*** is the corresponding distance of energy transport from the source in the same time *t*.

Figure 3 shows a schematic of a wavefront as the group-velocity surface multiplied by the traveltime *t*. The grey areas of the wavefront in this figure represent the leading edge of the low-amplitude region of figure 2. The grey regions come from the edges of the transducer, as seen in the distribution of group-velocity vectors in figure 3. The bolder vectors that show the travel of the plane-wave portion of the wavefront are parallel and there is a high concentration of energy in this plane-wave portion since there is no geometrical spreading in the propagation of a plane wave. One can see from this geometry that if the traveltime is measured by observing the arrival of the grey area of this wavefront, the raypath used when calculating the group velocity cannot be assumed to be a line between the centres of the transducers.

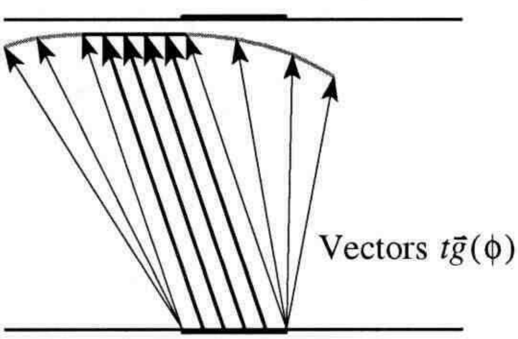

FIG. 3. The wavefront as represented by the group-velocity surface $\boldsymbol{g}(\phi)$ multiplied by the traveltime *t*. Note that the grey areas, the regions outside the plane-wave portion of the wavefront, are first arrivals from the edges of the transducer.

METHOD

In a numerical investigation of the measurements made on the phenolic block, the wavefield is calculated in the same way as in figure 2 in order to determine what sort of velocity is obtained from the division of transducer separation by traveltime. When calculating the position of the wavefront emanating from the transducer, the transducer is divided up into small discrete elements; a wavefront is calculated for each element and these are then summed over the source transducer.

In acquiring the wavefront for each element, the group- or ray-velocity surface is calculated. The wavefront is then assumed as the group-velocity surface scaled by the traveltime. Using the ray-velocity surface as the wavefront is called the ray approximation and is valid as a far-field approximation in homogeneous media. In order to derive the group-velocity surface, Christoffel's equation is solved for the phase velocity. This equation is an eigensystem of the form

$$\Gamma \mathbf{A} = \rho v^2 \mathbf{A}$$

The tensor Γ is real and symmetric, thereby giving real and positive eigenvalues which are equal to the density times the square of the phase velocity (ρv^2), and the eigenvectors are the respective polarization vectors $\mathbf{A}$. Γ is defined as a function of the elastic constants of the material, c_{ijkl}, and the unit wavefront-normal vector $\mathbf{n}$, as follows:

$$\Gamma_{ik} = c_{ijkl} n_j n_l;$$

$$i,j,k,l = 1,2,3.$$

Once the phase-velocity surface is known, where v is the magnitude and $\mathbf{n}$ defines the direction of the phase-velocity vector, the group-velocity surface can be derived. Since the traveltime measurements for the purpose of deriving the elastic constants are performed in assumed symmetry planes, the angle between group and phase velocity is confined to that plane. The two-dimensional relationship between the group velocity, g, and phase-velocity, v, in symmetry planes is given by many authors (e.g. Postma 1955; Brown et al., 1991; Dellinger 1991) as

$$g = \sqrt{v^2 + \left(\frac{\partial v}{\partial \theta}\right)^2},$$

where θ is the angle between the phase vector $\boldsymbol{v}$ in a symmetry plane and the symmetry axis with the slower direction of P-wave travel. The group angle ϕ in this plane is given by

$$\phi = \theta + \arctan\left[\frac{(\partial v/\partial \theta)}{v}\right].$$

In the computer program written for this study, the group-velocity surface is calculated once and then that surface is added into the data grid for each element of the source. Geometrical spreading is approximated by the inverse of the distance travelled along a given raypath. The resulting wavefront is convolved with a Ricker wavelet with a dominant frequency of approximately 600 kHz which is the dominant frequency of the transducers used in the laboratory experiments on the orthorhombic medium (Cheadle et al., 1991). The transducers were sized at 12.6 mm in diameter, the phenolic cube was assumed 10 cm across each side and 11.55 cm across the diagonal directions between bevelled edges. The elastic constants and density of the material were taken from the same paper.

The resulting plots are of a wavefront in the plane of symmetry that has travelled roughly 98% of the distance from source to receiver in the quasi-compressional (qP) and quasi-shear (qS_1 and qS_2) cases. The same elapsed time was used for qS_1 and qS_2. From here it can be interpreted whether or not the traveltime recorded between source and receiver represents the group or the phase velocity across the sample. The program also calculates the angle between the group velocity and the direct path between source and receiver which is normal to both transducer faces in these experiments.

RESULTS AND DISCUSSION

Model Plots

Plots were generated for qP, qS_1 and qS_2 waves for six propagation directions in the sample, that is along each symmetry axis and along the three diagonal directions in symmetry planes at 45° from the symmetry axes. For example, the measurement direction between the *x* and *y* axes at 45° to each axis is referred to as the *xy* direction. In this study, the *x, y, z, yz, zx,* and *xy* directions correspond to the 1, 2, 3, 4, 5 and 6 directions of Cheadle et al. (1991).

Figure 4 shows a triad of plots for the more straightforward case which is the measurement along a symmetry axis. These plots are cross-sections in the *zx* plane with the *x* axis running vertically between source and receiver. In these plots, where the measurement of seismic wave propagation is along a symmetry axis, the group and phase velocities are equivalent, as mentioned earlier. The question of whether group or phase velocity or neither is being determined arises when the experiment is carried out in the off symmetry directions

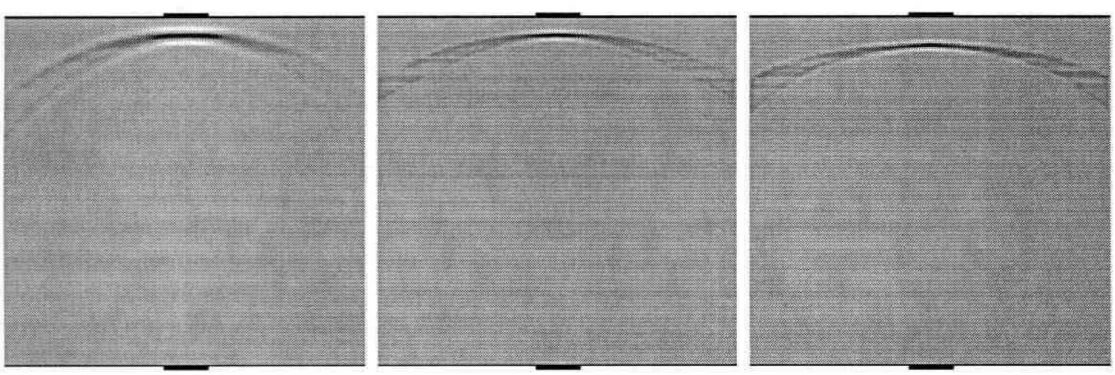

qP qS_1 qS_2

FIG. 4. Three wave types propagating along the *x* axis. an axis of symmetry.

An interesting example of the off-symmetry measurement is the wave propagation in the *zx* plane. The *x* and *z* axes are the directions of highest and lowest qP-wave velocity so this symmetry plane displays the greatest anisotropy. Figure 5 shows the wavefront plot triad for the measurement in the *zx* direction.

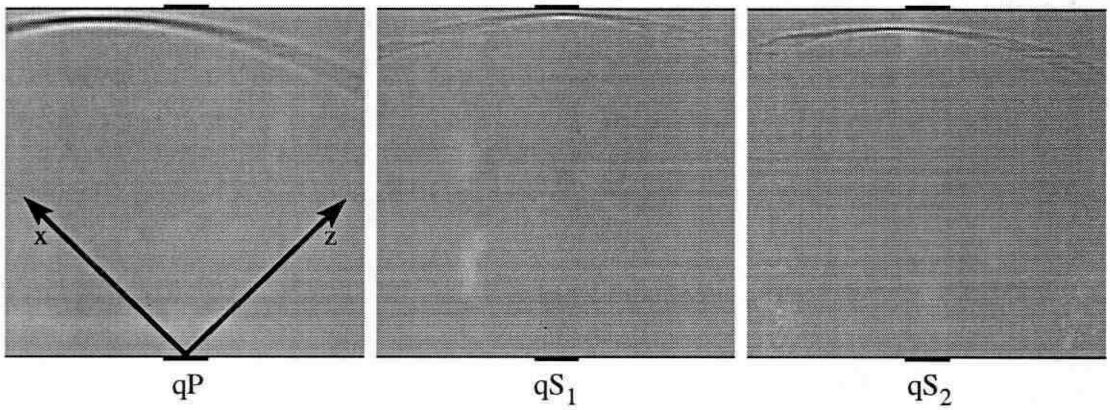

FIG. 5. Propagation in the *zx* plane. Coordinate axes are shown in the qP-wave plot.

It can be seen here (figure 5) that the group and phase velocities are not equivalent in this measurement direction. The flat plane-wave portion of the wavefront for the qP-wave is moving to the left, just as was seen in figure 2. The difference between this wavefront and that in figure 2 is caused by the difference in the size of the transducers. Here in this figure, the transducers are 12.6 mm in diameter which is significantly smaller than the 40 mm diameter transducers that are used in figure 2. Using this smaller transducer, it appears that the plane-wave portion of the wavefront does not hit the receiver transducer. One can conclude from figure 5 that to determine the qP wave group velocity, the correct distance of travel to be used is the distance from the right edge of the source to the left edge of the receiver.

In the qS-wave cases, there is less anisotropy observed than in the qP-wave cases and it appears that the phase velocity will be measured for these polarizations in this measurement direction. The plane-wave portion of the wavefront will be observed as the first impulse at the receiver transducer and therefore the distance across the sample divided by the traveltime observed will yield the correct phase velocity.

For the *yz* plane, there is a little less observable anisotropy than appears in the *zx* plane. The *z* direction is normal to the layers of fabric and is the direction with the lowest qP velocity, 2925 m/s, which is substantially lower than the qP velocity in either *x* or *y* axis, 3576 m/s and 3365 m/s respectively. The *y*-axis velocity is 15% greater than the *z*-axis velocity which is less than the 22% difference between the qP velocities along the *x* and *z* axes.

The plots, shown here in figure 6, show that there will be a phase velocity measured for both qS_1 and qS_2 and a possible group velocity for the qP wave. Here there is some question as to which of group or phase-velocity will be measured for the qP polarization. The edge of the plane-wave portion may be observed at the receiver. Is there a region on the wavefront where neither group nor phase-velocity is measured? This could be true if we always used the distance between centres of transducer faces in calculating velocity, without thinking any further, but this is not necessary; group velocity can always be calculated from the measured traveltime, even with finite transducers: there is, however, an uncertainty in the length of the raypath which has to be resolved. This will be further discussed below using geometrical arguments.

What can be concluded from these plots is that the quasi-shear-wave measurements will directly yield a phase velocity and the qP-wave measurement will likely give a group velocity.

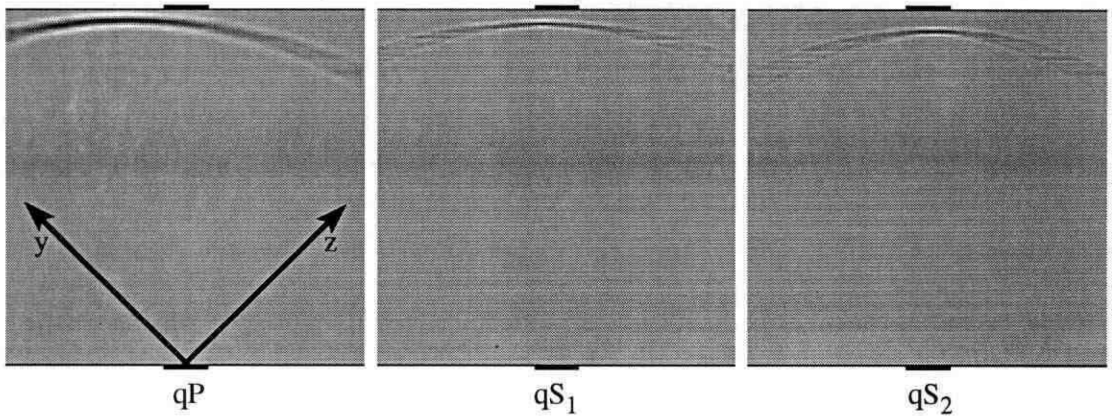

FIG. 6. Propagation in *yz* plane. The coordinate axes are shown in the qP-wave plot.

The last diagonal measurement is in the *xy* plane where the velocity anisotropy is due to the different type of the weave of the fabric. The least qP-wave anisotropy is observed in this plane where the difference between qP-wave velocities is only 6%. From the plots of the wavefronts propagating in this symmetry plane (figure 7), it can be assumed that the traveltime across the sample representing the phase velocity is measured. In each case, there will be an arrival of the plane-wave portion of the wavefront at some part of the receiver. Note that in this plane, the shear-wave splitting is relatively large as shown by the difference in the distance travelled by the two wave types. In this case, the qS_2 has its particle polarization in a direction near vertical or close to the *z* direction which is the slowest direction in this sample.

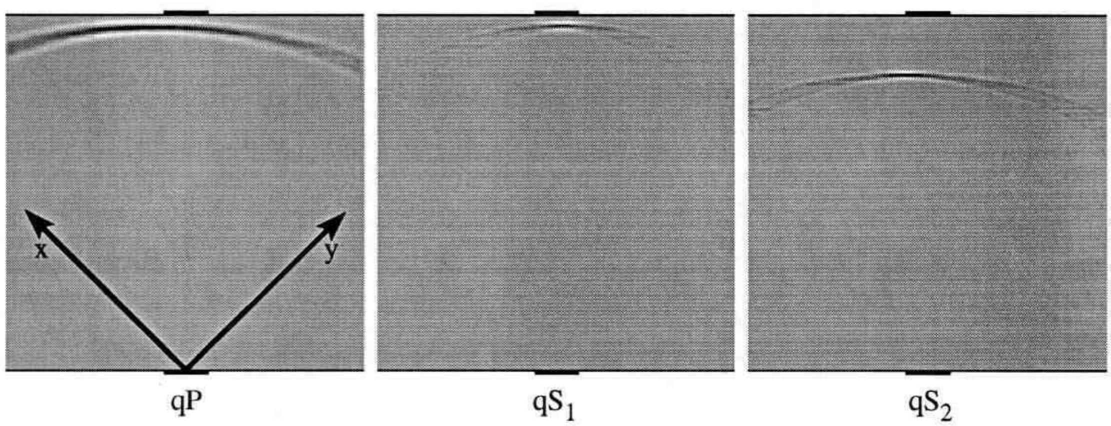

FIG. 7. Propagation in *xy* plane. The coordinate axes are shown in the qP-wave plot.

From the plots of the wavefronts in the sample of Phenolic CE, it has been observed that in most cases the phase velocity has been measured except when there is a large velocity anisotropy as with the qP-wave measurement in the *zx* and *yz* directions. In this case the traveltime measurement may be indicative of a group velocity. If the medium displayed more pronounced anisotropy than what has been observed here, then one could be confident that these measurements would, indeed, yield group velocity.

Geometry

One other form of output from this analysis is the angles between the group and phase-velocity vectors. This is also the angle between the group-velocity vector and the normal to the transducer faces. This angle will indicate where the edge of the plane-wave portion of the wavefront is.

Consider a seismic wave propagating from a source transducer in a symmetry plane in a direction such that the angle between the group- and phase-velocity vectors, δ, is equal to δ_m. Figure 8a shows a wavefront propagating from the transducer at the bottom of the figure and the associated plane phases. The plane phases and the plane-wave portion of the wavefront are in black. Figure 8b defines the angle δ_m as the maximum angle between the group and phase velocities where there will be some plane-wave observed at the receiver. From the geometry of the figure, this maximum angle is given by:

$$\delta_m = \arctan\left(\frac{\text{transducer diameter}}{\text{height of sample}}\right). \tag{1}$$

It is apparent that from this illustration, that when δ is greater than δ_m none of the planar wavefront portion will be observed at the receiver. Rather, the receiver in this case will be illuminated only by the curved grey area of the wavefront (figure 7a) which is a group-velocity surface. This grey portion of the wavefront to the right of the black plane-wave portion comes from the very edge of the transducer which, when considering the first arrival of energy, behaves like a point source. A group velocity is obviously measured in this case, but the raypath is not $\boldsymbol{v}t$ (figure 8b), the distance between the faces of the transducers, but is $\boldsymbol{g}t$, the oblique raypath from the right edge of the source transducer to the left edge of the receiver transducer.

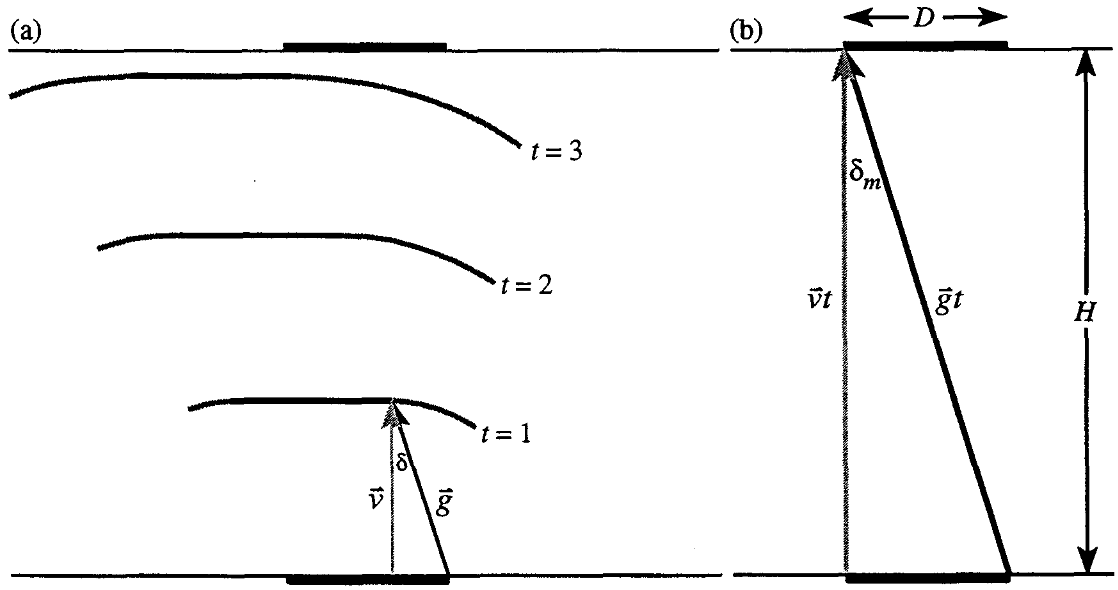

FIG. 8. The geometric model for the phase -velocity measurement limit. Plot (a) shows group-velocity surfaces at progressive unit time steps (time units arbitrary). The curved portions of the wavefronts beyond the planar segments are shown in grey. Plot (b) shows the geometry of this limiting case with the graphical definition of the maximum group-to-phase angle δ_m.

Once the angle δ becomes greater than δ_m, the measured traveltime is no longer indicative of the phase velocity. In this case, the velocity, if determined by dividing the normal transducer separation by the traveltime, will be something between phase and group velocity as indicated by Dellinger (1992). But if one is able to determine the actual distance travelled in the oblique ray or group direction, one will be able to calculate the group velocity. The maximum such distance, corresponding to $\delta = \delta_m$, will be

$$\sqrt{D^2 + H^2}\ .$$

Therefore, the maximum difference, ε, between this and the normal separation will be

$$\varepsilon = \sqrt{D^2 + H^2} - H.$$

One can see from this equation that for large samples and small transducers, this pathlength difference goes to zero and, in effect a group traveltime will always be measured without worry of transducer effects. The maximum raypath length error for the experimental geometry used in this study is fairly small compared to the size of the 115.5 mm sample at $\varepsilon = 0.7$ mm.

Table 1 shows the angle between group and phase velocity from this modelling study. Additional data in this table are the percentage differences between the group and phase velocities. This table shows that there is very little difference in the magnitudes of the group and phase velocities in the off-symmetry directions of this medium; there is a maximum near 2% for the qP wave in the *zx* direction.

Using equation (1), δ_m is calculated as 6.22° for H = 115.5 mm and D = 12.6 mm. The only waves for which $\delta > \delta_m$ are the qP waves measured in the *zx* and *yz* directions. From the analysis of the plots, it was determined that all but these two wave measurements would be measuring phase-velocity. This geometrical analysis is fast and simple and appears to agree with the conclusions made from the interpretation of the wavefront plots.

		xy direction		*zx* direction		*yz* direction	
		angle	%difference	angle	%difference	angle	%difference
Wave Type	qP	4.11	0.257%	11.63	2.053%	8.49	1.096%
	qS1	0.63	0.006%	0.57	0.005%	0.98	0.015%
	qS2	1.65	0.041%	2.62	0.105%	0.68	0.007%

Table 1. Table of the angle between the group- and phase-velocity vectors in degrees for the three off axis directions. The "% difference" figure is a measure of the difference between the magnitudes of the group and phase velocities.

Cheadle et al. (1991, p1608) calculated the phase angle which, when subtracted from the group angle, 45°, yields the angle δ. With this information and equation (1), which gives δ_m as a function of the experimental geometry, this geometrical analysis could have been applied to determine whether group or phase velocities were measured by comparing calculated δ values with δ_m.

An important conclusion may be drawn from this geometrical analysis of the propagation of the wavefront. For elastic property determination, it is desirable to measure phase velocity between the source and receiver. If large source and receiver transducers are used, then the experimentalist can be confident that it is, indeed, a traveltime that will yield the phase velocity in the normal direction between transducer faces. With finite area source and receiver transducers, there will always be some uncertainty, not only in the distance that the wave has travelled at the group velocity, but also in the calculated group velocity direction. In measuring properties of anisotropic materials where the seismic velocities change with direction, this directional error may be significant.

APPLICATION TO EXPERIMENTAL DATA

We use the information about the measurement of phase velocity in the experiment performed by Cheadle et al. (1991) to recalculate stiffnesses from the measured phase velocities.

We used the same method as outlined in the appendix with one important difference: the traveltime divided by the normal separation is assumed to yield phase velocity and not group velocity. This procedure then has one less step in it, namely the estimation of phase velocities from the group velocities; the stiffnesses are calculated directly from the phase velocities. The new calculations need only to be made on those stiffnesses dependent on the diagonal measurements, since there is no difference between group and phase velocity along a symmetry axis.

The results of these calculations show what little effect the difference between group and phase velocity has on the calculation of stiffnesses of the phenolic. The average difference between phase velocities determined in the two studies is 0.4%. This results in even smaller differences in the stiffnesses. From table 2, it is apparent that there is not one case where the stiffness calculated is different from the previously calculated stiffness to four significant figures. There are some differences in the individual calculated stiffness, but the average of the stiffnesses calculated using qP- and qSV-wave velocities are essentially identical.

	Stiffnesses x 10^9			
	Assuming Group		Assuming Phase	
	Stiffness	Average	Stiffness	Average
C_{12} (qP)	7.104		7.103	
C_{12} (qSV)	7.462	7.283	7.462	7.283
C_{13} (qP)	6.258		6.258	
C_{13} (qSV)	7.008	6.633	7.009	6.633
C_{23} (qP)	6.097		6.096	
C_{23} (qSV)	6.662	6.379	6.662	6.379

Table 2. Table of the stiffnesses calculated assuming group velocity (from Cheadle et al., 1991) and assuming phase velocity. The two calculations of each stiffness come from the qP and qSV arrival times (see Cheadle et al. for details).

CONCLUSIONS

From the interpretation of wavefront plots based on a ray model and from geometrical arguments it has been shown that, for most cases in the off-symmetry directions, Cheadle et al. have measured phase velocity in the orthorhombic medium. The effects caused by assuming group velocity were seen to be relatively small in that the difference between group and phase velocity of this medium is 2% or less.

The small (<2%) difference between two sets of phase velocities used in calculating the stiffnesses in the Phenolic CE made an insignificant difference when the stiffnesses were calculated. The calculation of the off-diagonal stiffnesses from the phase velocities is not very sensitive to small changes in the diagonal traveltimes.

A geometrical argument defined a maximum angle between group and phase velocity vectors for which the phase traveltime can be observed. In this case, the geometrical analysis yielded the same results with regard to the question of group or phase velocities as did the modelling study. This geometric method is a fast and easy way to determine which velocity type may be directly calculated from the traveltimes.

Future work will be done in pursuit of this type of geometrical analysis. Once the geometry of the wave propagation between finite transducers is better understood, perhaps there can be a geometrical correction that will correct for the error in the group velocity that is calculated from a 'near-phase' traveltime. This would entail determining the raypath of the first arriving energy at the receiver transducer using an analysis based on the geometry of the experiment and the angle δ as it changes with the ray direction.

REFERENCES

Brown, R.J., Lawton, D.C. and Cheadle, S.P. (1991) "Scaled physical modelling of anisotropic wave propagation: multioffset profiles over an orthorhombic medium" Geophys. J. Int. **107**, 693-702.

Cheadle, S.P., Brown, R.J. and Lawton, D.C. (1991) "Orthorhombic anisotropy: a physical seismic modelling study" Geophysics **56**, No. 10, 1603-1613.

Dellinger, J. (1992) "Do core sample measurements record group or phase velocity?" 62nd Ann. Internat. Mtg., Soc. Expl. Geophy., Expanded Abstracts, 662-665.

Dellinger, J. (1991) "Anisotropic seismic wave propagation" Ph.D. thesis, Stanford University.

Postma, G.W. (1955) "Wave propagation in a stratified medium" Geophysics **20**, 780-806.

Press, W. H., Flannerty, B.P., Teukolsky, S.A., and Vetterling, W.T. (1988) *Numerical Recipes in C*, Cambridge U. P.

Shuvalov, L. A. (1981) *Modern Crystallography IV: Physical Properties of Rocks*, Springer-Verlag, Berlin.